Eur. Phys. J. B **25**, 439–443 (2002)
DOI: 10.1140/epjb/e20020050

THE EUROPEAN PHYSICAL JOURNAL B
EDP Sciences

Electron transport properties of MgB_2 in the normal state

M. Putti[1,a], E. Galleani d'Agliano[1], D. Marrè[1], F. Napoli[1], M. Tassisto[1], P. Manfrinetti[2], A. Palenzona[2], C. Rizzuto[3], and S. Massidda[4]

[1] INFM/CNR, Dipartimento di Fisica, Via Dodecaneso 33, 16146 Genova, Italy
[2] INFM, Dipartimento di Chimica e Chimica Industriale, Via Dodecaneso 31, 16146 Genova, Italy
[3] Dipartimento di Chimica e Chimica Industriale, Via Dodecaneso 31, 16146 Genova, Sincrotrone di Trieste, Trieste
[4] INFM Dipartimento di Fisica, Università di Cagliari, S.P. Monserrato-Sestu Km 0.700, 09042 Monserrato (CA), Italy

Received 16 November 2001 and Received in final form 21 December 2001

Abstract. We report measurements of the resistivity, ρ, and the Seebeck coefficient, S, of a MgB_2 sintered sample, and compare S with theoretical calculations based on precise electronic structure calculations. ρ is fitted well by a generalized Bloch-Grüneisen equation with a Debye temperature Θ_R of 1050 K. S is given by the sum of a diffusive and a phonon drag term and the behavior in the temperature region $T_c < T < 0.1\Theta_R$ follows the relationship $AT + BT^3$. The phonon drag term indicates a strong electron-phonon interaction. The diffusive term, compared with calculations, suggests that σ bands give the main contribution to the Seebeck effect.

PACS. 74.25.Fy Transport properties (electric and thermal conductivity, thermoelectric effects, etc.) – 72.15.Jf Thermoelectric and thermomagnetic effects – 74.70.Ad Metals; alloys and binary compounds (including A15, Laves phases, etc.)

The discovery of 40 K superconductivity in MgB_2 [1] has stimulated a large discussion on the nature of the pairing and many evidences suggest a BCS-type mechanism: the isotope effect on T_c [2], energy gap [3] and specific heat measurements [4] and a negative pressure coefficient of T_c [5,6].

Electron transport properties may give insight into the normal state conduction process, on the electronic structure and on the electron-phonon interaction. From this point of view, the MgB_2 behaves like a simple metal; in fact the resistivity is described by Bloch-Grüneisen equation [7,8], the magnetoresistivity follows a generalized Kohler's rule [9,7] and the Seebeck effect [5,6,10–12] is small, positive and nearly linear. In the picture of simple metal the Seebeck effect was analyzed considering only a diffusive term linear with temperature, but the extrapolation of this term to zero temperature yields an unphysical non-vanishing negative value. This inconsistency can be eliminated taking a phonon drag term into account as suggested in reference [13]; this contribution, moreover, is expected to be remarkable in a metal with strong electron-phonon coupling.

In this paper we analyze the thermopower (TEP) measurements as the sum of a diffusive and a phonon drag terms and we show that our data, as well as data from literature, are compatible with a phonon drag term of the expected order of magnitude. The linear diffusive term, vanishing with temperature, is then compared with a calculation that we perform based on the precise electronic structure.

We present resistivity and TEP measurements on a sintered MgB_2 sample. The compound MgB_2 was prepared by direct synthesis from the elements: Mg and crystalline B were well mixed together and closed by arc welding under pure argon into outgassed Ta crucibles which were then sealed in quartz ampoules under vacuum. The samples were slowly heated up to 950 °C and maintained at this temperature for 1 day. X-ray diffraction shows values of the lattice parameters, $a = 3.087(1)$, $c = 3.526(1)$ Å, and the absence of extra reflections. The specimen for transport measurements has been prepared by pressing the powders in a stainless-steel die into a pellet which was then sintered by heat treatment at 1000 °C for 2 days.

The resistivity measurements were performed using a standard four probe technique and the TEP was measured using an a.c. technique described elsewhere [14] with sensitivity of 0.5% and accuracy of 1.5%. The gradient applied to the sample was varied from 1 to 3 K/cm and the frequency from 0.003 to 0.008 Hz; the data were acquired with a slowly rising temperature (1 mK/sec).

The resistivity measurements are presented in Figure 1 up to 300 K; the transition region is enlarged in the inset. The critical temperature defined at half of the transition is $T_c = 38$ K with amplitude $\Delta T_c \sim 0.3$ K. The residual resistivity ratio (RRR = $\rho(300\text{ K})/\rho(40\text{ K})$) is 3, whereas

[a] e-mail: putti@fisica.unige.it

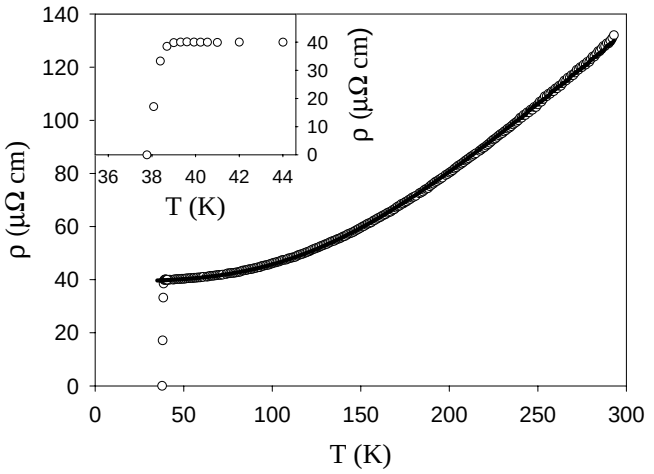

Fig. 1. ρ as a function of temperature; the transition region is enlarged in the inset. The best fitting curve is reported as a continuous line.

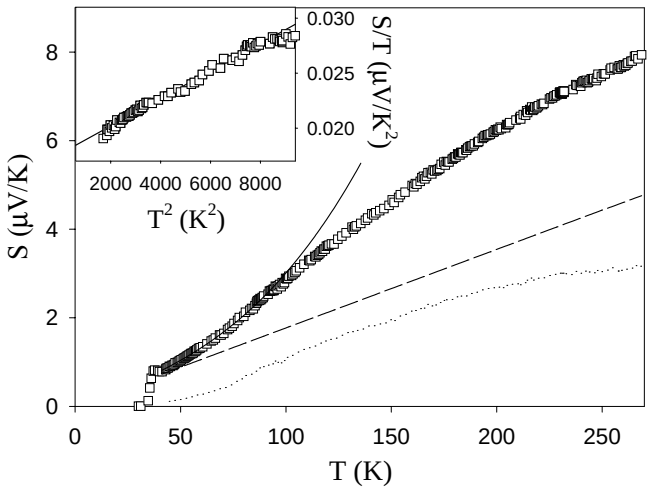

Fig. 2. S as a function of temperature; the continuous line is given by equation (6) with $A = 1.76 \times 10^{-2}$ μV/K^2 and $B = 1.26 \times 10^{-6}$ μV/K^4; the dashed line is $S_d = AT$; the dotted line is $S - S_d$. In the inset it is shown S/T as a function of T^2; the continuous line is the best fit performed in the range 2000 K^2 $< T^2 <$ 8000 K^2.

the resistivity at $T = 40$ K is 40 $\mu\Omega$cm. The critical temperature somehow lower than the maximum value for this compound could be related to non perfect stoichiometry of Mg in the sintered sample, as suggested in reference [7]. In this framework, we can explain the rather large residual resistivity in terms of scattering with the Mg vacancies as well as with the grain boundaries [15]. Anyway, reference [7] concludes that also in non perfect stoichiometry sintered samples the resistivity temperature dependence may be considered as basically intrinsic, independent on granularity. Thus we fit the temperature dependence of the normal state resistivity to the expression:

$$\rho(T) = \rho_0 + \rho_{\rm ph}(T), \tag{1}$$

where ρ_0 is the temperature-independent residual resistivity and $\rho_{\rm ph}(T)$ the phonon-scattering contribution assumed of the generalized Bloch-Grüneisen form:

$$\rho_{\rm ph}(T) = (m-1)\rho'\Theta_R \left(\frac{T}{\Theta_R}\right)^m \int_0^{\Theta_R/T} \frac{z^m {\rm d}z}{(1-{\rm e}^{-z})({\rm e}^z-1)}, \tag{2}$$

where Θ_R is the Debye temperature, ρ' is the temperature coefficient of resistivity for $T \gg \Theta_R$ and $m = 3-5$. Equation (2) reduces to $\rho(T) = \rho_0 + \text{const.} \times T^m$ for $T \ll \Theta_R$; indeed from 40 to 100 K the resistivity is well fitted by a power law with $m = 2.9 - 3.4$ [7–9], while lower m values are found when the fit is extended up to room temperature. The best fit of equations (1–2) to our data is obtained with $m = 3$, $\rho_0 = 39.7$ $\mu\Omega$cm, $\Theta_R = 1050$ K, $\rho' = 0.49$ $\mu\Omega$cm/K and is shown in Figure 1 as a continuous line. The Θ_R value is in fair agreement with $\Theta_{\rm D}$ obtained from heat capacity measurements [16] although lower values ($700 - 900$ K) have also been reported [4]. ρ' which is proportional to the dimensionless $\lambda_{\rm tr}$ coupling coefficient, has the same value that in A15 compounds [17], consistent with a moderately strong coupling.

The TEP measurements are shown in Figure 2, where we see the transition around 38 K and a continuous increase, with curvature changing from positive to negative above 150 K. In contrast to resistivity, whose values and temperature dependence are strongly influenced by sample structural quality, TEP measurements seem to be less affected by disorder or granularity, as well proved in cuprates [18]. Indeed, all the data reported in literature show always almost identical behaviors. Looking to TEP data in more details, a difference among TEP measurements, is in the temperature dependence below 100 K. While in many references TEP measurements show a linear behavior below 100 K, in some other papers [5,12] as well as our data, they show instead a light positive curvature. This curvature will be discussed in the following.

The observed temperature behavior can be analyzed considering first the diffusive contribution to S given by the Mott formula:

$$S_d = \frac{\pi^2}{3}\frac{K_{\rm B}^2 T}{e}\frac{\sigma'}{\sigma}, \tag{3}$$

where e is electronic charge, σ is the electrical conductivity and $\sigma' = \frac{\partial}{\partial\varepsilon}\sigma(\varepsilon)\mid_{\varepsilon_{\rm F}}$. Note that $\varepsilon_{\rm F}$ must be counted upward for electrons and downward for holes. In the isotropic case and if the relaxation time τ is independent of energy (this is the case for scattering with grain boundaries), $\sigma'/\sigma = 3/2\varepsilon_{\rm F}$, independent of the scattering processes and equation (3) becomes:

$$S_d = \frac{\pi^2}{2e}\frac{K_{\rm B}^2 T}{\varepsilon_{\rm F}}\,. \tag{4}$$

Second, we must consider a phonon drag term S_g, arising for temperatures lower than the Debye temperature, when the phonon relaxation time for interaction with other phonons and impurities is much longer than the relaxation

Table 1. The coefficients A and B obtained by fitting S/T *vs.* T^2 (Eq. (6)); Θ_D as obtained by equation (8); ε_F as obtained by equation (7).

	A (μV/K^2)	B (μV/K^4)	Θ_D (K)	ε_F (eV)
MgB_2	1.76×10^{-2}	1.26×10^{-6}	1430	2.1
MgB_2 [5]	1.70×10^{-2}	1.30×10^{-6}	1430	2.2
MgB_2 [10,13]	2.00×10^{-2}	1.30×10^{-6}	1430	1.8
$Mg_{0.95}Al_{0.05}B_2$ [10,13]	2.88×10^{-2}	1.41×10^{-6}	1390	1.3
$Mg_{0.9}Al_{0.1}B_2$ [10,13]	2.99×10^{-2}	1.49×10^{-6}	1360	1.2

time for phonon-electron interactions. For pure isotropic metals and considering only electron-phonon normal processes, an upper bound for S_g can be roughly estimated to be given [19]

$$S_g = \frac{C_{ph}}{3ne}, \tag{5}$$

where C_{ph} is the phonon specific heat per unit volume. Thus, for $T \ll \Theta_D$, and assuming S_g to really reach this upper bound, the total TEP S will take the form:

$$S = S_d + S_g = AT + BT^3, \tag{6}$$

where:

$$A = \frac{\pi^2 K_B^2}{2e} \frac{1}{\varepsilon_F} \tag{7}$$

$$B = \frac{\beta_3}{3ne} = \frac{K_B}{e} \frac{1}{n_a} \frac{4\pi^4}{5} \frac{1}{\Theta_D^3}\,. \tag{8}$$

Here $\beta_3 = \frac{9NK_B}{\Theta_D^3}$ is the coefficient of the low temperature phonon specific heat, N is the number of atoms per unit volume, and n_a is the number of valence electrons. Equation (6) can be compared with the experimental TEP of MgB_2 in the temperature range $T_C < T < 0.1\Theta_D \sim$ 100 K showing a good overlap with a large part of our measurements.

The inset of Figure 2 shows the ratio S/T as a function of T^2 for 40 K $< T <$ 100 K. The data show a linear behavior up to a T^2 value of 8000 (T = 90 K) and then begin to bend. The best fit performed in the range 2000 K^2 $< T^2 <$ 8000 K^2 is plotted as a continuous line and the fit parameters are $A = 1.76 \times 10^{-2}$ μV/K^2 and $B = 1.26 \times 10^{-6}$ μV/K^4.

In Figure 2 equation (6) with A and B given by the fit is plotted as a continuous line, while the diffusive term $S_d = AT$ is plotted as a dashed line. The experimental curve is well fitted by equation (6) up to 100 K, above which the data change curvature and tend to increase linearly, with nearly the same slope of S_d. The experimental phonon drag term defined as $S - S_d$, plotted as a dotted line, tends to saturate above 250 K. This is exactly what it is expected for S_g; in fact, increasing the temperature, phonon-impurity and phonon-phonon processes become more important, and the phonon drag falls, causing a peak in the TEP. In metals as Cu, Ag, Au, Al, the phonon drag peak occurs at about $\Theta_D/5$ [19], while in our case the peak is not yet reached at $\Theta_D/4$ giving a further evidence of the importance of the electron-phonon coupling in MgB_2.

We therefore find that the diffusive and phonon drag terms contribute nearly equally to the TEP. The previous reports [5,6,10,12] and [13] which consider only a diffusive term non-vanishing with temperature, can be analyzed taking also a phonon drag contribution into account. We fitted the data of references [5,10,13] to the equation (6) and we found coefficients A and B, summarized in Table 1, in good agreement with those obtained with our data. The main difference among samples is the temperature range in which the T^3 behavior extends; this range is wider in our data and in data of reference [5] where a positive curvature below 100 K is evident.

To further verify the consistency of the model, let us try now to relate the coefficient A and B with some microscopic parameters. We first start neglecting the multiband character of MgB_2 and we pursue in our naive model of isotropic free electrons. Its reliability will be discussed afterwards in the light of the band structure effects.

The coefficients A and B of our sample, and those extrapolated from data in literature for pure [5] and Al doped MgB_2 [10,13], are summarized in Table 1. The Fermi energy ε_F and the Debye temperature Θ_D are obtained directly from A and B (Eqs. (7, 8)): $\Theta_D \sim 1400$ K, is in good agreement with Θ_R (only the 30% higher) considering that equation (5) is an overestimation of S_g; ε_F for pure MgB_2 is of the order of 2 eV and becomes 1.2 eV for Al doped samples: since the Al doping raises the Fermi level, the decreasing of ε_F with Al doping is a further evidence (in addition to the positive sign) that S_d is dominated by holes.

Let us now turn to the TEP as resulting from the band structure of MgB_2. Two types of bands contribute to the conduction [20,21]: two σ bands, deriving from the $p_{x,y}$ states of B and two π bands deriving from the p_z states with very different dimensional character, the σ bands being of hole-type and nearly 2D, and the 3D π bands mainly of electron-type. Great relevance in the discussion of the pairing mechanism has been given to the σ bands [21], and the positive sign of the Hall coefficient and of the TEP, as well as the increasing of the latter with Al doping, confirm the importance of these bands in the transport properties. Starting from the precise electronic structure calculations described in reference [20], we have computed the Seebeck tensor S_d, as a function of the chemical potential shift, to reproduce within a rigid band scheme the Al doping. These calculations are performed using the scheme described, *e.g.*, in references [20,22]. Because of hexagonal symmetry, the independent components are $S_{xx} = S_{yy}$

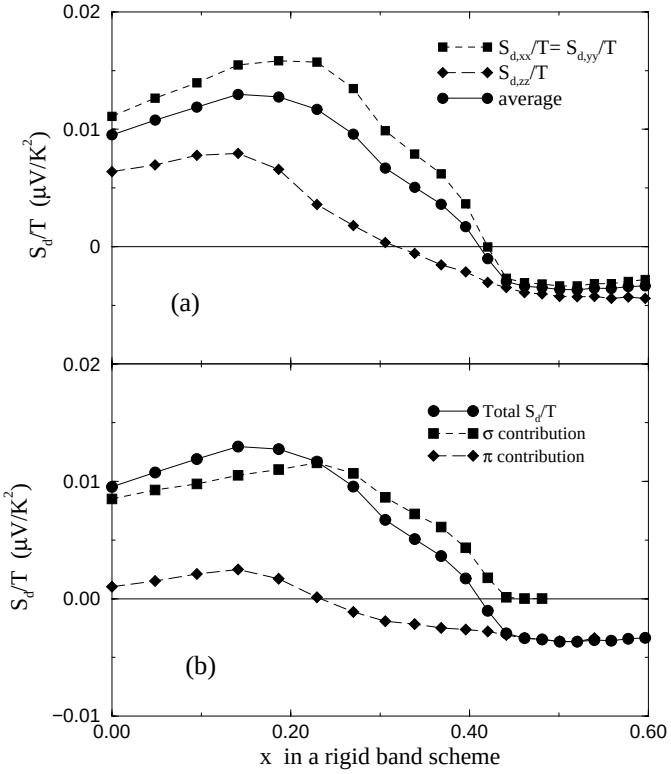

Fig. 3. S_d/T as a function of doping, estimated in a rigid band scheme from the integrated DOS. (a) Tensor components and average; (b) Average S_d/T and its band decomposition, as explained in the text.

and S_{zz}. Briefly, if Ω is the unit cell volume and $v_i(\mathbf{k}, n)$ are the cartesian components of the Fermi velocities for the nth band, we obtain the TEP components S_{ii} as:

$$S_{ii}(T) = \frac{K_{\mathrm{B}}}{e} \frac{\int \mathrm{d}\varepsilon \frac{(\varepsilon-\mu)}{K_{\mathrm{B}}T} \sigma_{ii}(\varepsilon) \left(-\frac{\mathrm{d}f}{\mathrm{d}\varepsilon}\right)}{\int \mathrm{d}\varepsilon \sigma_{ii}(\varepsilon) \left(-\frac{\mathrm{d}f}{\mathrm{d}\varepsilon}\right)} \tag{9}$$

where

$$\sigma_{ij}(\varepsilon) = \frac{e^2}{\Omega} \sum_{\mathbf{k},n} v_i(\mathbf{k}, n) v_j(\mathbf{k}, n) \tau(\mathbf{k}, n) \delta(\varepsilon(\mathbf{k}, n) - \varepsilon). \tag{10}$$

If we consider τ to be isotropic and independent of energy, it will not affect the final result. As pointed out in reference [22], S_{ii} vanishes in the approximation $-\frac{\mathrm{d}f}{\mathrm{d}\varepsilon} = \delta(\varepsilon - \mu)$, and it would therefore be appropriate to include the energy dependence of τ as well. Unfortunately, it is not easy to obtain a consistent $\tau(\varepsilon)$ approximation, and we therefore use the most conservative, $\tau = \mathrm{const.}$, approach. As it is important to assess the functional dependence of S on T, however, we checked a different form of $\tau(\varepsilon)$, in particular $\tau(\varepsilon)$ proportional to $1/N(\varepsilon)$ as suggested by [22]. The numerical values of S_d change, but it results linear with temperature in the range of interest.

S_d shows the expected linear behavior as a function of temperature, and we therefore plot in Figure 3 S_d/T, as a function of the electron doping, in a rigid band scheme. Figure 3a gives the tensor components, while to compare with experiment we show in Figure 3b the average of S_d/T over directions, $\overline{S}_d/T$. Since both numerator and denominator in the definition of S_d/T contain a band summation, there is no clear cut distinction between the σ and π contributions. With this warning, in order to better understand our results, we decompose in Figure 3b $\overline{S}_d/T$ in terms of σ and π bands contributions (*i.e.* we decompose the numerator of Eq. (9)). We notice that for small values of doping the dominant, positive contribution comes from σ bands; when the chemical potential goes beyond the maximum energy of the σ-bonding band the A point ($\mathbf{k} = (0, 0, \frac{\pi}{c})$ this contribution disappears and the resulting S_d/T is much smaller and negative, identical to the π contribution. The smallness of the latter relative to the σ contribution can be easily understood: the numerator of equation (9) essentially monitors the $\sigma_{ii}(\varepsilon)$ derivative with respect to ε, and this quantity is much larger for the σ bands. As a function of the doping x, S_d/T initially grows, and then it bends down, especially because of the σ contribution when μ goes beyond the 2D to 3D crossover (position of the σ band at Γ), but also because of the π contribution change.

The calculated values are smaller, by a factor of about 1.7–2, than the experimental values of Table 1. The trend as a function of doping, however, is similar in experiment and theory; it would be interesting, in this respect, to obtain the experimental values for larger doping. While the agreement between the bare band theory value and experiment is not quantitatively good, it may considered to be satisfactory based on the following considerations: (i) our calculations do not include the energy dependence of τ, which may result into quantitative differences [22]. As a speculation, we may say the following: our understanding of MgB_2 indicates a strong electron-phonon coupling for the σ band top (mostly with the E_{2g} phonon mode). Very likely, such a strong coupling will depend on the energy location, relative to the σ band top, resulting into an energy dependent $\tau(\varepsilon)$. (ii) Also, our calculations do not contain any form of renormalization; it has been a controversial question, in the literature [23], whether renormalization should affect the bare band-structure results. If this would be the case, the strong electron-phonon coupling in MgB_2 would bring the theoretical value into agreement with experiment. Undoubtedly, the presence of contributions to TEP from different bands, having different electron-phonon couplings, should prevent any complete cancellation of renormalization effects in the final result.

In summary, we showed that resistivity and TEP in the normal state can described within an independent electron framework, by taking into account the high phonon frequencies and the strong electron-phonon coupling. In particular the TEP is the sum of a diffusive and a phonon drag terms which contribute nearly equally to it. The phonon drag term was not previously recognized, in fact its peak is shifted above room temperature by the high Debye temperature and the strong electron-phonon interaction. The diffusive term is positive and increases with Al doping.

The comparison of the experimental values with the theoretical ones, obtained from the precise electronic structure, suggests that bands give the main contribution to the TEP. Further investigation will be necessary to verify this result; in particular transport properties on samples with higher level of Al doping will be a useful tool to better investigate the role of the σ bands, whose relevance in the pairing mechanism has been strongly advocated.

This work was partially supported by the Italian Consiglio Nazionale delle Ricerche (CNR) through the "Progetto 5% Applicazioni della superconduttività ad alta T_c".

References

1. J. Nagamatsu, N. Nakagawa, T. Muranaka, Y. Zenitani, J. Akimitsu, Nature **63**, 410 (2001).
2. S.L. Bud'ko, G. Lapertot, C. Petrovic, C.E. Cunningham, N. Anderson, P.C. Canfield, Phys. Rev. Lett. **86**, 1877 (2001).
3. G. Karapetrov, M. Iavarone, W.K. Kwok, G.W. Crabtree, D.G. Hinks, Phys. Rev. Lett. **86**, 4374 (2001); A. Sharoni, I. Felner, O. Millo, Phys. Rev. B **63**, 220508R (2001).
4. W. Walti, E. Felder, C. Degen, G. Wigger, R. Monnier, B. Delley, H.R. Ott, Phys. Rev. B **64**, 172515 (2001); Y. Wang, T. Plackowsky, A. Junod, Physica C **355**, 179 (2001).
5. B. Lorenz, R.L. Meng, C.W. Chu, Phys. Rev. B **64**, 12507 (2001).
6. E.S. Choi, W. Kang, J.Y. Kim, Min-Seok Park, C.U. Jung, Heon-Jung Kim, Sung-Ik Li, `cond-mat/0104454`.
7. X.H. Chen, Y.S. Wang, Y.Y. Xue, R.L. Meng, Y.Q. Wang, C.W. Chu, Phys. Rev. B **65**, 025402 (2001), `cond-mat/0107154`.
8. A.V. Sologubenko, J. Jun, S.M. Kazakov, J. Karpinski, H.R. Ott, `cond-mat/0111273`.
9. D.K. Finnemore, J.E. Ostenson, S.L. Bud'ko, G. Lapertot, P.C. Canfield, Phys. Rev. Lett. **86**, 2420 (2001).
10. B. Lorenz, R.L. Meng, Y.Y. Xue, C.W. Chu, Phys. Rev. B **64**, 52513 (2001).
11. M. Schneider, D. Lipp, A. Gladun, P. Zahn, A. Handstein, G. Fuchs, S.-L. Drechsler, M. Richter, K.-H. Muller, H. Rosner, Physica C **363**, 6 (2001), `cond-mat/0105429`.
12. T. Muranaka, J. Akimitsu, M. Sera, Phys. Rev. B **64**, 020505R (2001).
13. B. Lorenz, Y.Y. Xue, R.L. Meng, C.W. Chu, `cond-mat/0110125`, *Presented at NATO Advanced Research Workshop "New Trends in Superconductivity", Yalta (Ukraine) 16-20 September, 2001.*
14. M. Putti, M.R. Cimberle, A. Canesi, C. Foglia, A.S. Siri, Phys. Rev. B **58**, 12344 (1998).
15. M. Putti, E. Galleani d'Agliano, D. Marrè, F. Napoli, M. Tassisto, P. Manfrinetti, A. Palenzona, *Studies of High temperature Supeconductors*, Vol. 38, edited by A.V. Narlikar (Nova Science Publisher, 2001), p. 303.
16. F. Bouquet, R.A. Fisher, N.E. Phillips, D.G. Hinks, J.D. Jorgensen, Phys. Rev. Lett. **87**, 047001 (2001).
17. F. Nava, O. Bisi, K.N. Tu, Phys. Rev. B **34**, 6143 (1986).
18. J.L. Tallon, J.R. Cooper, P.S.I.P.N. de Silva, G.V.M. Williams, J.W. Loram, Phys. Rev. Lett. **75**, 4114 (1995).
19. J.M. Ziman, *Electrons and phonons* (Oxford, Clarendon Press, 1960); R.D. Barnard, *Thermoelectricity in metals and alloys* (Taylor & Francis Ltd, London, 136, 1972).
20. G. Satta, G. Profeta, F. Bernardini, A. Continenza, S. Massidda, Phys. Rev. B **64**, 104507 (2001).
21. J. Kortus, I.I. Mazin, K.D. Belashenko, V.P. Antropov, L.L. Boyer, Phys. Rev. Lett. **86**, 4656 (2001); J.M. An, W.E. Pickett, Phys. Rev. Lett. **86**, 4366 (2001).
22. P.B. Allen, W.E. Pickett, H. Krakauer, Phys. Rev. B **37**, 7482 (1988).
23. G. Grimvall, *The electron-phonon interaction in metals*, edited by E.P. Wohlfarth, in *Selected Topics in Solid State Physics*, Vol. XVI (North-Holland, 1981); A.B. Kaiser, Phys. Rev. B **35**, 4677 (1987), and references therein.